J. Fluid Mech. (1968), *vol.* 34, *part* 4, *pp.* 687–703
Printed in Great Britain

Axisymmetric hypersonic flow with strong viscous interaction

By JOHN WEBSTER ELLINWOOD
AND HAROLD MIRELS
Aerospace Corporation, El Segundo, California

(Received 17 July 1967 and in revised form 22 April 1968)

Stewartson's theory for axisymmetric hypersonic flow of a model gas over slender bodies with strong viscous interaction and strong shock wave is extended to power-law viscosity variation and Prandtl numbers other than one. Flow properties at the body surface and shock are obtained without recourse to numerical integration. Numerical computations are presented for axisymmetric flow over a three-quarter power-law body with strong shock wave and viscous interactions that range from weak to strong.

1. Introduction

A slender axisymmetric body with local body radius $r_w(x)$, when situated in a steady hypersonic stream, disturbs the flow in a limited region known as the shock layer. If the flow has sufficient density ρ, the shock layer consists of a viscous boundary layer with characteristic thickness $\delta(x)$ adjacent to the body, an inviscid layer external to the boundary layer, and a surrounding shock wave. If, in addition, the flow speed is sufficiently great, the shock wave has limiting properties and is said to be strong. If also the body grows as $x^{\frac{3}{4}}$, the disturbed flow is self-similar in that it becomes a function of a single spatial variable (Yasuhara 1956). Generally, even the self-similar flow requires numerical description because of non-linearities in the mathematics.

Often of interest are situations in which $\delta/r_w \ll 1$. In such cases, the boundary layer is too thin to affect pressures in the shock layer and is equivalent to the boundary layer in a related, plane flow. However, as free-stream velocity is increased, frictional heating reduces boundary-layer densities and increases δ. At some speed, δ/r_w will no longer be negligible, and the boundary layer then interacts weakly with the pressure field. At even greater speeds, or for more slender bodies, it is expected that $\delta/r_w \gg 1$, in which case the boundary layer interacts strongly with the pressure field and the body slope retains only a minimal influence on pressure.

Figure 1 depicts hypersonic flow with strong viscous interaction over a slender, axisymmetric, three-quarter power-law body. The domain of self-similar flow is limited downstream (to the right) by weakness in the shock wave and upstream by rarefaction and related effects that are discussed in appendix A. In figure 1, the division of the boundary layer into a viscous convective layer and an inner viscous layer is the result of the limit $\delta/r_w \gg 1$. Such a division also characterizes

Lighthill 1950), as well as flow around a finite body at very low Reynolds number. incompressible flow along a slender cylinder (Stewartson 1955; Glauert & The layers shown in figure 1 also appear in flow over a body that does not grow as $x^{\frac{3}{4}}$.

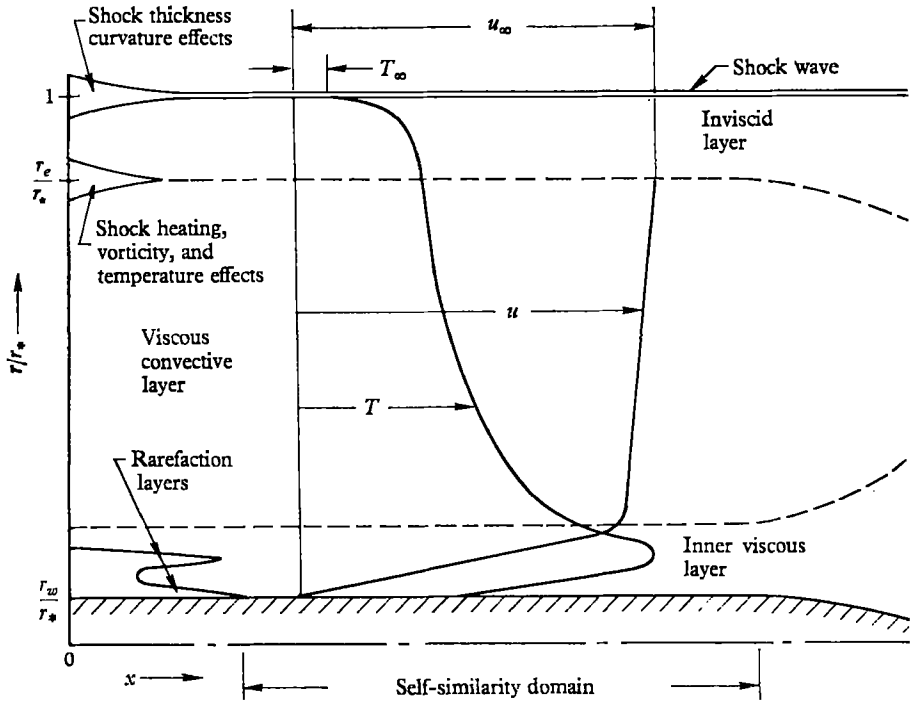

FIGURE 1. Sketch of u and T profiles and gas layers for strong viscous interaction on slender body in hypersonic flow ($r_w \sim x^{\frac{3}{4}}$, $r_e \equiv \delta^* + r_w$).

A theory for axisymmetric hypersonic flow with strong viscous interaction and a strong shock has been presented by Stewartson (1964), who considers a model gas near the nose of a sharp cone (or of any body, where $r_w \to x^n$ as $x \to 0$ and $n > \frac{3}{4}$). In this paper, we correct a manipulative error in Stewartson's results for the effect of surface temperature,† and we extend his solution to include gases with Prandtl number Pr other than one and with viscosity varying as the ω power of enthalpy h. The major boundary-layer properties are obtained in closed form without recourse to numerical integrations, and the domain of validity is defined (appendix A).

As a check on the accuracy of the strong-interaction theory, numerical solutions of the self-similar, axisymmetric boundary-layer equations were obtained for three-quarter power-law bodies and a strong shock. These machine solutions, which are of interest in their own right, are described in §4 and extend earlier computations by Yasuhara (1962) to stronger interactions, where comparisons can be made with the present strong-interaction theory.

† Stewartson's results for a model gas have been confirmed independently by Solomon (1967), who also corrects for the effect of surface temperature. (Solomon, in addition, presents a method of solution for model gases at finite speeds.)

2. General equations

The equations presented in this section are general in the sense that they apply both to strong viscous interaction over arbitrary slender axisymmetric bodies and to interaction of moderate strength over three-quarter power-law bodies.

The boundary-layer equations for axisymmetric flow are simplified by transformation of the cylindrical co-ordinates (x, r) to a modified form of the Lees–Dorodnitsyn (Lees 1956*a*) variables (ξ, η):

$$\xi = \int_0^x (\rho\mu)_w u_e r_w^2 dx, \quad \eta = u_e(2\xi)^{-\frac{1}{2}} \int_{r_w}^r \rho r dr. \tag{2.1}$$

Subscripts w and e denote values at the body surface and boundary-layer edge, respectively. The modifications are that r is no longer approximated by r_w in the integral for η and that the surface normal is taken to be directed radially. For slender bodies $(r_w^2/x^2 \ll 1)$, this slight rotation of axes alters neither the equations nor the boundary conditions in the leading approximation. Equation (2.1) is essentially the transformation used by Yasuhara (1962), but not by Stewartson (1964). Let the dependent variables be f, which is the integral of $(u/u_e)d\eta$; g, the stagnation enthalpy ratio H/H_e; and R, the spatial variable r^2/r_w^2. Then the equations for streamwise momentum, energy and continuity are:

$$0 = [(g - mf_\eta^2)^{\omega-1} g_w^{1-\omega} R f_{\eta\eta}]_\eta + ff_{\eta\eta} + \beta(g - f_\eta^2) - 2\xi(f_\eta f_{\xi\eta} - f_\xi f_{\eta\eta}), \tag{2.2}$$

$$0 = \{(g - mf_\eta^2)^{\omega-1} g_w^{1-\omega} R[g_\eta - 2(1-Pr)mf_\eta f_{\eta\eta}]\}_\eta + Prfg_\eta - 2Pr\xi(f_\eta g_\xi - f_\xi g_\eta), \tag{2.3}$$

$$R = 1 + A\int_0^\eta (g - mf_\eta^2)d\eta. \tag{2.4}$$

Functions only of ξ in (2.2)–(2.4) are m, which is a finite Mach number parameter; β, the pressure-gradient parameter; and A, the transverse-curvature parameter, which is later related to a viscous interaction parameter, Λ. For slender bodies where u_e is essentially constant, these parameters become

$$m = 1 - \frac{h_e}{H_e}, \quad \beta = -\frac{\gamma - 1}{m\gamma}\frac{d\log p_w}{d\log \xi}, \quad A = \frac{\gamma - 1}{m\gamma}\frac{u_\infty(2\xi)^{\frac{1}{2}}}{p_w r_w^2},$$

where γ is the specific heat ratio and p the pressure. If $A \ll 1$, then $R \approx 1$, and (2.2) and (2.3) then describe a thin, plane, Mangler boundary layer. We are concerned instead with cases where $A \gg 1$ (as in §3) or where A is of order one (as in §4).

We now restrict the discussion to hypersonic flows where $M_e^{-2} \ll 1$, and we set $m = 1$. This restriction is equivalent with the assumption that boundary-layer temperatures are elevated well above those in the inviscid layer. The body surface is assumed to be at constant temperature (which includes the insulated wall case). We further limit ourselves to either flows where the viscous interaction is strong [where generally $A = A(x)$] or flows where the body grows as $x^{\frac{3}{4}}$ with arbitrary interaction strength, in which case A is constant. For these cases, it

will be shown that the pressure decays as $(x \log A)^{-\frac{1}{2}}$. Then, within an error of order $1/\log A$ for the strong interaction case, ξ, β and A are these functions of x:

$$\xi = \frac{1}{\phi}\left(\frac{\gamma-1}{2} g_w M_\infty^2\right)^{\omega-1} \rho_\infty \mu_\infty u_\infty \frac{p_w}{p_\infty} r_w^2 x, \tag{2.5a}$$

$$\beta = \frac{\gamma-1}{2\phi\gamma}, \quad A = \frac{4}{(2\phi)^{\frac{1}{2}}} \frac{x}{g_w r_w}\left(\frac{\nu_\infty p_\infty}{u_\infty x p_w}\right)^{\frac{1}{2}} \left(\frac{\gamma-1}{2} g_w M_\infty^2\right)^{\frac{1}{2}(\omega+1)}, \tag{2.5b}$$

where ϕ is a function of x defined by

$$\phi \equiv \frac{d\log \xi}{d\log x} = \frac{d\log \int_0^x x^{-\frac{1}{2}} r_w^2 dx}{d\log x}. \tag{2.5c}$$

For power-law bodies ϕ is a constant. Note that $\nu_\infty = \mu_\infty/\rho_\infty$.

At the boundaries, it is assumed that slip and temperature jump are unimportant:

$$f(0) = f_\eta(0) = 0, \quad g(0) = g_w \quad \text{or} \quad g_\eta(0) = 0, \tag{2.6}$$

and that external vorticity is unimportant:

$$f_\eta \to 1, \quad g \to 1, \quad R_\eta \to 0 \quad \text{as} \quad \eta \to \infty. \tag{2.7}$$

The domain where these assumptions are valid is discussed in appendix A.

The transformed equations will produce values for $R(\infty)$, $f_{\eta\eta}(0)$, and either $g_\eta(0)$ or g_w. These can be related to displacement thickness δ^*, surface pressure, viscous interaction parameter, skin friction, and heat transfer rate or recovery temperature as follows. The axisymmetric definition of δ^* (Moore 1952) is

$$\int_{r_w}^{r_w+\delta^*} \rho_e u_e r\, dr = \int_{r_w}^{\infty} (\rho_e u_e - \rho u) r\, dr.$$

For hypersonic flows, δ^* and the boundary-layer thickness δ differ by an amount that vanishes as $M_e^{-2} \to 0$, for all degrees of interaction, and r is bounded as $\eta \to \infty$. It follows that

$$\delta^*/r_w = \delta/r_w = [R(\infty)]^{\frac{1}{2}} - 1. \tag{2.8}$$

It is now necessary to obtain a measure of the surface pressure. The pressure throughout the boundary layer and at the surface is the inner limit of pressures in the outer, inviscid layer (figure 1). Equations for the inviscid layer are nonlinear, but in the hypersonic small-disturbance limit considered here similarity solutions exist if the effective body ordinate r_e grows as certain powers of x, of which only the three-quarter power is of present interest. The three-quarter power-law inviscid solution has been evaluated numerically for $\gamma = 7/5$ by Valesko *et al.* (see Chernyi 1961, pp. 87, 244) and for γ from 1 to 5/3 by Kubota (see Hayes & Probstein 1966, p. 73). For a three-quarter power-law body (studied in § 4), this inviscid similarity solution is clearly applicable. On the other hand, for strong viscous interaction (studied in § 3) it will be shown that $r_e \sim \delta^*$ grows as $x^{\frac{3}{4}}[\log A(x)]^{-\frac{1}{4}}$. The inviscid partial differential equations in this case can be expanded in inverse powers of $\log A(x)$. The equations of leading order have the same form and solution as those for constant A (i.e. the three-quarter power-law body case). The error incurred by using only the leading term in the proposed

asymptotic expansion is of the higher order $(\log A)^{-1}$. Combination of (2.8) with these numerical results for p_e/p_* and r_e/r_*, where stars denote evaluation immediately behind the shock at the same x, leads to

$$p_w/p_\infty = (jM_\infty r_w/x)^2 R(\infty), \tag{2.9}$$

where
$$j \equiv \frac{3}{2}\left[\frac{\gamma}{2(\gamma+1)}\frac{p_e}{p_*}\right]^{\frac{1}{2}}\frac{r_*}{r_e} = \begin{cases}0{\cdot}846, & \gamma = 1{\cdot}4,\\ 0{\cdot}941, & \gamma = 1{\cdot}67.\end{cases}$$

Also
$$\frac{r_e}{r_*} = \begin{cases}0{\cdot}875, & \gamma = 1{\cdot}4,\\ 0{\cdot}819, & \gamma = 1{\cdot}67.\end{cases}$$

Let a viscous interaction parameter $\Lambda(x)$ be introduced by the definition

$$\Lambda \equiv (x^2/r_w^2) M_\infty^\omega (\rho_\infty u_\infty x/\mu_\infty)^{-\frac{1}{2}}. \tag{2.10a}$$

Λ is used to characterize the viscous interaction because δ/r_w varies as Λ for weak interactions, because both parameters are large for strong interactions, and because Λ is a grouping of known parameters, whereas δ/r_w is not. Substitution of (2.9) into (2.5*b*) yields a relation for Λ in terms of the transformed variables and A:

$$\Lambda = \frac{j}{4}\left[\left(\frac{2}{\gamma-1}\right)^{\omega+1} 2\phi g_w^{1-\omega} R(\infty)\right]^{\frac{1}{2}} A. \tag{2.10b}$$

The skin friction coefficient is

$$C_f \equiv \frac{2(\mu\,\partial u/\partial r)_w}{\rho_\infty u_\infty^2} = j\left(\frac{\gamma-1}{2}g_w\right)^{\frac{1}{2}(\omega-1)}\left(\frac{r_w}{x}\right)^3 \Lambda f_{\eta\eta}(0)[2\phi R(\infty)]^{\frac{1}{2}}. \tag{2.11}$$

Assuming $C_f \sim r_w^{-1}$, as will be shown in (3.26), and $p_w \sim x^{-\frac{1}{2}}$, we find that the total drag coefficient referred to base area πr_b^2 is

$$C_D(L^2/r_b^2) = 2j\left(\frac{\gamma-1}{2}g_w\right)^{\frac{1}{2}(\omega-1)}\{\Lambda f_{\eta\eta}(0)[2\phi R(\infty)]^{\frac{1}{2}}\}_b + \frac{3j^2R(\infty)}{\gamma}, \tag{2.12}$$

where L is the body length and $\Lambda_b = (r_b/L)^{-2} M_\infty^\omega (\rho_\infty u_\infty L/\mu_\infty)^{-\frac{1}{2}}$ and where the pressure-drag contribution (last term in right member of equation (2.12)) applies for $n = \frac{3}{4}$ only. The heat transfer rate to the wall is

$$q \equiv \frac{(\mu\,\partial H/\partial r)_w}{Pr} = \frac{\rho_\infty u_\infty^3}{4Pr}\lambda C_f, \tag{2.13}$$

where $\lambda \equiv g_\eta(0)/f_{\eta\eta}(0)$. λ is referred to later as a Reynolds analogy parameter and is constant for an isothermal wall if either $\Lambda \gg 1$ or Λ is constant, the two cases to be considered in §§ 3 and 4, respectively.

3. Analytic solution for $\Lambda \gg 1$

In the strong-interaction limit the interaction parameter Λ, the transverse-curvature parameter A and δ/r_w are all very large. In this limit the boundary layer for any slender axisymmetric body can be divided into two viscous layers (as in figure 1, which displays a three-quarter power-law body). One is an inner layer adjacent to the body where convective and pressure effects are unimportant. It is in the inner layer that the velocity and stagnation enthalpy profiles are principally developed. The other viscous layer is an outer, convective layer. In

this layer velocity and stagnation enthalpy depart from corresponding values in the free stream by only small amounts, and convective and pressure terms, as well as the shear term, must be retained in the viscous equations. Other layers shown in figure 1 are not important in the régime of the present theory.

(a) *Inner viscous layer*

It will be shown, (3.13) and (3.22*b*), that $f_{\eta\eta}(0)$ is of order $A/\log A$. Hence, in the immediate vicinity of the wall, f and η may be taken to be of order A^{-1} (to within a factor $\log A$) while R, f_η and g are of order A^0. Substituting this ordering into (2.2) and (2.3) and neglecting terms of order A^{-2}, one finds that only the first term needs to be retained in each right member. The reduced equations correspond to Couette flow, and integration with boundary conditions (2.6) yields

$$g_w^{\omega-1} f_{\eta\eta}(0) = (g - f_\eta^2)^{\omega-1} R f_{\eta\eta}, \tag{3.1}$$

$$\lambda g_w^{\omega-1} f_{\eta\eta}(0) = (g - f_\eta^2)^{\omega-1} R[g_\eta - 2(1-Pr) f_\eta f_{\eta\eta}]. \tag{3.2}$$

The inner viscous layer is defined as the region for which (3.1) and (3.2) are applicable. With increase in η, the error associated with these equations is of order η/A. Hence (3.1) and (3.2) can be considered valid for η less than order A^1. (When η is of order A^0, so are f, f_η and g, while R is of order A^1.)

Elimination of R and another integration provides an enthalpy integral:

$$g = g_w + \lambda f_\eta + (1-Pr) f_\eta^2. \tag{3.3}$$

Since h/H_e is simply $g - f_\eta^2$ in this approximation, whenever $\lambda > 0$ the temperature peak occurs within the boundary layer and has the value

$$(h/H_e)_{MT} = g_w + \lambda^2/(4Pr) \quad \text{at} \quad f_\eta = \lambda/(2Pr). \tag{3.4}$$

The Reynolds analogy parameter λ is a function of g_w and Pr. It will be shown that $\lambda \leqslant Pr$. Equations (2.4), (3.1) and (3.3) provide the velocity profile and η:

$$\log R = g_w^{1-\omega} A[f_{\eta\eta}(0)]^{-1} \int_0^{f_\eta} (g_w + \lambda t - Prt^2)^\omega dt, \tag{3.5}$$

$$\eta = g_w^{1-\omega}[f_{\eta\eta}(0)]^{-1} \int_0^{f_\eta} R(g_w + \lambda t - Prt^2)^{\omega-1} dt. \tag{3.6}$$

The known constants are Pr, ω and either g_w or λ, all of order A^0, and the indefinitely large parameter A. The unknowns are a constant of order A^0 (either λ or g_w) and $f_{\eta\eta}(0)$. These are evaluated by matching the flow in the inner viscous layer with that in the viscous convective layer.

(b) *Viscous convective layer*

In the viscous convective layer, the terms representing the effects of viscous shear no longer dominate the equations of motion. With all terms retained and with $m = 1$, (2.2) and (2.3) become, after integration with (2.6),

$$f_{\eta\eta}(0) = (g - f_\eta^2)^{\omega-1} g_w^{1-\omega} R f_{\eta\eta} + \beta \int_0^\eta (g - f_\eta^2) d\eta + f_\eta (1 + 2\xi \partial/\partial\xi) f - (1 + 2\xi \partial/\partial\xi) \int_0^\eta f_\eta^2 d\eta, \tag{3.7}$$

$$\lambda f_{\eta\eta}(0) = (g-f_\eta^2)^{\omega-1} g_w^{1-\omega} R[g_\eta - 2(1-Pr) f_\eta f_{\eta\eta}] + Pr\left[g(1+2\xi\partial/\partial\xi)f - (1+2\xi\partial/\partial\xi)\int_0^\eta f_\eta g\, d\eta\right]. \quad (3.8)$$

If $f_{\eta\eta}(0)$ is of order $A/\log A$ as assumed, the terms in (3.7) are of comparable size only if η and f are of order A, and R is of order A^2, with possible factors of $\log A$. If these scalings are properly chosen, (3.7) and (3.8) reduce to ordinary differential equations in terms of a new independent variable ζ, where ζ is of order one in this layer. It will be seen that the following replacements are appropriate.

(i) Variables:

$$\eta = \zeta A\epsilon^\omega \phi, \quad \xi = \xi, \quad (3.9)$$

$$R = \bar{R}(\zeta) A^2 \epsilon^{\omega+1} \phi[1+O(\epsilon)], \quad (3.10)$$

$$f_\eta = 1 - \epsilon F_\zeta(\zeta) + O(\epsilon^2), \quad (3.11)$$

$$g = 1 - \epsilon G(\zeta) + O(\epsilon^2), \quad (3.12)$$

where $\epsilon = \epsilon(\xi)$ cannot be chosen until properties of the inner and convective viscous layers are matched. (It will be found that ϵ is $\log A$ raised to a negative power.) Assume without loss of generality that $F(\infty) = 0$.

(ii) Operators:

$$\partial/\partial\eta = (\zeta/\eta)\partial/\partial\zeta,$$

$$\xi\partial/\partial\xi = \xi\partial/\partial\xi - [d\log(\eta/\zeta)/d\log\xi]\zeta\partial/\partial\zeta,$$

where, noting $A\phi$ varies like $x/\xi^{\frac{1}{2}}$, (2.5), and neglecting derivatives of ϵ and $\log A$ (i.e. neglecting terms of order ϵ)

$$d\log(\eta/\zeta)/d\log\xi = -\tfrac{1}{2} + 1/\phi.$$

(iii) Parameters:

$$\lambda = \lambda_0[1+\epsilon\lambda_1 + O(\epsilon^2)], \quad (3.13a)$$

$$f_{\eta\eta}(0) = A\epsilon^{\omega+1} f_0[1+O(\epsilon)], \quad (3.13b)$$

$$\int_0^\infty f_\eta(1-f_\eta)\,d\eta = A\epsilon^{\omega+1}\phi f_1[1+O(\epsilon)], \quad (3.14a)$$

$$\int_0^\infty f_\eta(1-g)\,d\eta = A\epsilon^{\omega+1}\phi g_1[1+O(\epsilon)], \quad (3.14b)$$

$$\int_0^\infty (g-f_\eta^2)\,d\eta = A\epsilon^{\omega+1}\phi r_1[1+O(\epsilon)]. \quad (3.14c)$$

Equations (3.14) follow from the fact that the major contributions to each integral occurs in the viscous convective layer.

With these replacements, equations (3.7), (3.8) and (2.4) become to leading order:

$$f_0 = -(2F_\zeta - G)^{\omega-1} g_w^{1-\omega} \bar{R} F_{\zeta\zeta} + 2f_1 + [(\gamma-1)/(2\gamma)]\bar{R} + 2(F - \zeta F_\zeta), \quad (3.15a)$$

$$\lambda_0 f_0 = -g_w^{1-\omega}(2F_\zeta - G)^{\omega-1}\bar{R}[G_\zeta - 2(1-Pr)F_{\zeta\zeta}] + Pr\left(2g_1 + 2\int_\infty^\zeta G\,d\zeta - 2\zeta G\right), \quad (3.15b)$$

$$\bar{R} = r_1 + 2F - \int_\infty^\zeta G\,d\zeta. \quad (3.15c)$$

An alternate equation, involving only $\bar{R}$, can be obtained. Multiply (3.15a) by $2Pr$ and subtract (3.15b). The result, using (3.15c), is

$$(2Pr-\lambda_0)f_0 = -g_w^{1-\omega}\bar{R}_\zeta^{\omega-1}\bar{R}\bar{R}_{\zeta\zeta}+2Pr\{(2f_1-g_1-r_1)+[(3\gamma-1)/(2\gamma)]\bar{R}-\zeta\bar{R}_\zeta\}. \tag{3.16}$$

At the outer edge of the boundary layer,† (2.7) and (3.10) indicate

$$\bar{R}_\zeta(\infty) = F_\zeta(\infty) = G(\infty) = 0.$$

Specifically, as $\zeta\to\infty$, $\zeta\bar{R}_\zeta$, ζF_ζ and ζG vanish algebraically if $\omega < 1$ [as noted by Bush (1966) for plane flow] and exponentially if $\omega \geqslant 1$. Even here where $\delta/r_w \gg 1$, the outer edge of the axisymmetric boundary layer behaves as that for plane flow, in the hypersonic limit. Equations (3.15) become as $\zeta\to\infty$

$$f_0 = 2f_1+[(\gamma-1)/(2\gamma)]\bar{R}(\infty), \tag{3.17a}$$

$$\lambda_0 f_0 = Pr(2g_1), \tag{3.17b}$$

$$\bar{R}(\infty) = r_1. \tag{3.17c}$$

At the inner edge of the viscous convective layer $\bar{R}$ must vanish, from the scaling (3.9) and (3.10), and the convective terms in (3.16) and (3.15) must vanish. Thus

$$0 = \bar{R}(0), \qquad 0 = 2f_1-g_1-r_1, \tag{3.18a}$$

$$0 = f_1+F(0), \quad 0 = g_1+\int_\infty^0 G\,d\zeta. \tag{3.18b}$$

Equations (3.17) and (3.18) provide $\bar{R}(\infty)$ in terms of the unknowns f_0 and λ_0:

$$\bar{R}(\infty) = [\gamma/(3\gamma-1)]f_0(2Pr-\lambda_0)/Pr. \tag{3.19}$$

Further matching of the convective layer with the inner layer is now considered in order both to demonstrate the validity of the present two-layer approximation and to provide explicit expressions for λ_0, f_0 and ϵ. As $\zeta\to 0$, since $\bar{R}\bar{R}_{\zeta\zeta}/\bar{R}_\zeta$ can be written as $d\bar{R}_\zeta/d\log\bar{R}$, (3.16) becomes

$$-[g_w^{1-\omega}/(\omega+1)]\bar{R}_\zeta^{\omega+1} = (2Pr-\lambda_0)f_0\log\bar{R}+O(\bar{R}^0). \tag{3.20}$$

By dividing (3.16) by (3.15a) in the limit $\zeta\to 0$ and noting (3.15c), it is found that

$$2Pr-\lambda_0 = 2-\frac{dG}{dF_\zeta} = \frac{d\bar{R}_\zeta}{dF_\zeta}. \tag{3.21}$$

The inner viscous-layer solution (3.3) for $g(f_\eta)$, expanded in terms of G and F_ζ and truncated after order ϵ, matches (3.21) if

$$\lambda_0 = Pr-g_w. \tag{3.22a}$$

† As a consequence of assuming that $g-mf_\eta^2$ is proportional to $2F_\zeta-G$, we need to strengthen the requirement that $M_e^{-2} \ll 1$ and require instead $M_e^{-2} \ll \epsilon \ll 1$. In this case the velocity components, pressure, and stagnation enthalpy in the viscous convective layer can be matched to their inviscid-layer counterparts, but the temperature, density, and Mach number cannot (Bush 1966). This last difficulty does not alter the boundary conditions proper for the outer edge of the viscous convective layer, noted above.

Similarly, expansion of (3.5) in terms of $\bar{R}$ and f_0 to leading order provides

$$\epsilon = (\log A)^{-1/(\omega+1)}, \quad f_0 = \tfrac{1}{2} J g_w^{1-\omega}, \tag{3.22b}$$

where

$$J \equiv \int_0^1 (g_w + Prt)^\omega (1-t)^\omega dt. \tag{3.23}$$

Special values of J are

$$J = \begin{cases} \frac{1}{6}(Pr + 3g_w), & \omega = 1, \\ (Pr)^\omega B(\omega+1, \omega+1), & g_w = 0, \\ 4(Pr)^\omega B(\omega+1, \omega+1), & g_w = Pr. \end{cases}$$

$B(\omega+1, \omega+1)$ is the Beta function and equals $\frac{1}{6}$ for $\omega = 1$ and 0·2540 for $\omega = \frac{3}{4}$. An approximate expression for J is

$$J \approx [\tfrac{1}{6}(Pr + 3g_w)]^\omega, \tag{3.24}$$

with an error less than 4% when $0{\cdot}5 < \omega \leqslant 1$.

Matching $\eta(f_\eta)$ from (3.6) with a relation not shown for $\zeta(F_\zeta)$ can be accomplished but contributes no new information. The assumptions that ϵ was $\log A$ to a negative power and that $f_{\eta\eta}(0)$ was of order $A/\log A$ have now led to a consistent analysis. In particular, substitution of (3.22) into (3.15)–(3.21) confirms that ζ is a similarity variable for the viscous convective layer, since no functions of ξ appear.

If field properties within the viscous convective layer are required, it is necessary to solve this initial-value problem numerically. In particular, Stewartson (1964) found $\bar{R}(\zeta)$ for $Pr = \omega = 1$ and $\gamma = \frac{7}{5}$ from (3.16), (3.18*a*) and (3.20). F and G can be computed from (3.15*a*) and (3.15*b*) using initial conditions

$$F(0) = -f_1 = J g_w^{1-\omega} \left[\frac{(1-5\gamma)Pr + (\gamma-1)g_w}{8(3\gamma-1)Pr} \right],$$

$$\int_\infty^0 G d\zeta = -g_1 = -J g_w^{1-\omega} [(Pr - g_w)/(4Pr)],$$

$$F_\zeta = (Pr + g_w)\bar{R}_\zeta = \tfrac{1}{2}(\bar{R}_\zeta + G), \quad \zeta \to 0,$$

obtained from (3.17) to (3.22). If, however, one is content with a solution for the inner viscous layer and integral boundary-layer properties, one need only collect formulae already obtained. Combining (2.10*b*), (3.10), (3.13), (3.19) and (3.22), we find that

$$R(\infty) = \frac{4}{j} \left[\frac{J\gamma}{3\gamma-1} \left(\frac{\gamma-1}{2} \right)^{\omega+1} \frac{Pr + g_w}{Pr} \right]^{\frac{1}{2}} \frac{\Lambda}{(\log \Lambda^2)^{\frac{1}{2}}} \tag{3.25a}$$

and

$$f_{\eta\eta}(0)[2\phi R(\infty)]^{\frac{1}{2}} = \frac{8J}{j} g_w^{\frac{1}{2}(1-\omega)} \left(\frac{\gamma-1}{2} \right)^{\frac{1}{2}(1+\omega)} \frac{\Lambda}{\log \Lambda^2}. \tag{3.25b}$$

From (2.10*b*), Λ and A are related by

$$\Lambda = \frac{j\phi}{4} g_w^{1-\omega} \left[\frac{\gamma J}{3\gamma-1} \left(\frac{2}{\gamma-1} \right)^{\omega+1} \frac{Pr + g_w}{Pr} \frac{1}{\log A} \right]^{\frac{1}{2}} A^2, \tag{3.25c}$$

so that Λ is of order $A^2/(\log A)^{\frac{1}{2}}$. With this information, all boundary-layer parameters can be expressed in closed form.

(c) *Properties at the wall and shock*

The boundary-layer edge and shock-wave locations are

$$\delta = r_w[R(\infty)]^{\frac{1}{2}}; \quad r_* = (r_*/r_e)\, r_w[R(\infty)]^{\frac{1}{2}}. \tag{3.26a}$$

The surface pressure ratio is

$$\frac{p_w}{p_\infty} = 4j\left[\frac{\gamma J}{3\gamma-1}\left(\frac{\gamma-1}{2}\right)^{\omega+1}\frac{Pr+g_w}{Pr}\right]^{\frac{1}{2}} M_\infty^{2+\omega}\left[\frac{\nu_\infty}{u_\infty x \log\Lambda^2}\right]^{\frac{1}{2}}. \tag{3.26b}$$

The skin friction coefficient is

$$C_f = 8J\left(\frac{\gamma-1}{2}\right)^{\omega}\left(\frac{r_w}{x}\right)^3\frac{\Lambda^2}{\log\Lambda^2}. \tag{3.26c}$$

The drag coefficient is due to friction, since the pressure-drag coefficient varies as the square root of the friction-drag coefficient, which is large compared with one. Note that $C_f \sim (r_w)^{-1}$, as previously assumed; therefore, drag per unit length is constant:

$$C_D\left(\frac{L^2}{r_b^2}\right) = 16J\left(\frac{\gamma-1}{2}\right)^{\omega}\left(\frac{\Lambda^2}{\log\Lambda^2}\right)_b. \tag{3.26d}$$

Lastly, the heat transfer rate is

$$q = \rho_\infty u_\infty^3 C_f(Pr-g_w)/(4Pr). \tag{3.27}$$

Equations (3.25)–(3.26) show that $p \sim (x\log\Lambda)^{-\frac{1}{2}}$ and that $r_e \sim \delta \sim x^{\frac{3}{4}}(\log\Lambda)^{-\frac{1}{4}}$, consistent with the corresponding *a priori* assumptions for (2.5) and (2.9). The pressure, friction, and heat transfer at any x are unaffected by the arbitrary body thickness at any other x, in that the function $\phi(x)$ does not appear in these expressions.

When γ is $\frac{7}{5}$ and ω is one, (3.26) reduces to:

$$\delta/r_w = 0{\cdot}849[(Pr+g_w)(Pr+3g_w)/(8Pr)]^{\frac{1}{4}}\Lambda^{\frac{1}{2}}(\log\Lambda^2)^{-\frac{1}{4}}, \tag{3.28}$$

$$r_*/r_w = 0{\cdot}971[(Pr+g_w)(Pr+3g_w)/(8Pr)]^{\frac{1}{4}}\Lambda^{\frac{1}{2}}(\log\Lambda^2)^{-\frac{1}{4}}, \tag{3.29}$$

$$p_w/p_\infty = 0{\cdot}517[(Pr+g_w)(Pr+3g_w)/(8Pr)]^{\frac{1}{2}}M_\infty^3(u_\infty x\log\Lambda^2/\nu_\infty)^{-\frac{1}{2}}, \tag{3.30}$$

$$C_f = (\tfrac{16}{15})[(Pr+3g_w)/4](r_w/x)^3\Lambda^2/\log\Lambda^2. \tag{3.31}$$

When Pr is one, (3.27)–(3.31) are Stewartson's (1964) results, except for corrections in the brackets for the effects of wall temperature. Stewartson anticipated that departures from model-gas properties would not differ seriously from his results. It is now clear that when the wall is either cold or insulated both C_f and q vary as Pr^ω and surface pressure varies as $Pr^{\frac{1}{2}\omega}$.

The present results indicate the correction to apply to $\omega = 1$ solutions for shear, heat transfer and displacement to account for $\omega \neq 1$. From (3.25) to (3.26), it is seen that $\nu_\infty/u_\infty x$, in the $\omega = 1$ solution, is replaced by $C\nu_\infty/u_\infty x$, where

$$C = (\mu_r/\mu_\infty)(T_\infty/T_r) \tag{3.32}$$

and T_r is a reference temperature defined by $T_r/T_0 = (J/J_1)^{1/(\omega-1)}$. Here $J_1 \equiv (J)_{\omega=1}$ and T_0 is the free-stream stagnation temperature. With the approximation (3.24),

$$T_r/T_0 \approx (Pr+3g_w)/6. \tag{3.33}$$

Cheng, Hall, Golian & Hertzberg (1961) derived (3.33) for the special case $Pr = 1$ and two-dimensional boundary layers. The reference viscosity, $\mu_r = \mu(T_r)$, is seen to correspond to an average value in the boundary layer, where the average is taken with respect to velocity (i.e. $J \sim \int \mu\, du$).

4. Numerical solution of self-similar equations when $\Lambda = O(1)$

When the body grows as $x^{\frac{3}{4}}$, when the shock wave is strong, and when the viscous interaction is of finite strength, the flow is self-similar but requires numerical computations. Equations (2.2)–(2.4), without the $\partial/\partial\xi$ terms and with both m and ω equal to one, have been integrated numerically as a two-point boundary-value problem by Yasuhara (1962) for $A \leqslant 10$ where either $\beta + \frac{1}{14}$ or $g_w = Pr = 1$. Additional computations have now been done for those cases where $\beta = \frac{1}{14}$, $Pr = 1$ or 0·7, either g_w or $g_\eta(0)$ vanish, and $A = 0$, 1, 5, 10, 100, 10^3, or 10^5. In each case it was possible to find a solution that satisfied all the

Pr	g_w	λ	A	$f_{\eta\eta}(0)$	$\frac{R(\infty)-1}{A}$	$\frac{\Lambda}{A}$	$\left(\frac{h}{H_e}\right)_{\max}$
1	1	0	0	0·5557	1·558	2·115	1
1	1	0	1	0·7578	1·934	3·623	1
1	1	0	5	1·3625	3·094	8·584	1
1	1	0	10	1·9705	4·291	14·02	1
1	1	0	100	9·409	18·76	91·64	1
1	1	0	10^3	59·60	114·7	716·5	1
1	1	0	10^5	3369	6301	53,096	1
1	0	0·9671	0	0·4909	0·4357	2·115	0·238
1	0	0·9687	1	0·5360	0·4757	2·569	0·239
1	0	0·9729	5	0·6983	0·6185	4·280	0·240
1	0	0·9758	10	0·8765	0·7759	6·260	0·241
1	0	0·9843	100	3·115	2·744	35·10	0·243
1	0	0·9885	10^3	17·616	15·489	263·3	0·245
1	0	0·9919	10^5	918·6	805·6	18,985	0·246
0·7	0·8308	0	0	0·5464	1·4426	2·115	0·8308
0·7	0·8166	0	1	0·7183	1·7458	3·505	0·8166
0·7	0·7984	0	5	1·2286	2·6905	8·041	0·7974
0·7	0·7904	0	10	1·7379	3·655	12·96	0·7904
0·7	0·7700	0	100	7·841	15·202	82·49	0·7700
0·7	0·7578	0	10^3	48·05	90·37	635·9	0·7578
0·7	0·7447	0	10^5	2624	4819	46,430	0·7447
0·7	0	0·7148	0	0·4871	0·3743	2·115	0·187
0·7	0	0·7150	1	0·5224	0·4034	2·506	0·187
0·7	0	0·7154	5	0·6510	0·5109	3·988	0·185
0·7	0	0·7156	10	0·7935	0·6288	5·710	0·185
0·7	0	0·7154	100	2·587	2·117	30·85	0·185
0·7	0	0·7138	10^3	13·999	11·655	228·4	0·182
0·7	0	0·7110	10^5	703·0	594·4	16,308	0·180

TABLE 1. Numerical results for self-similar axisymmetric hypersonic flows ($\omega = 1$, $\gamma = \frac{7}{5}$, $r_w \sim x^{\frac{3}{4}}$)

boundary conditions and for which f increased monotonically with η. Overshoot in $g(\eta)$ was exhibited in all insulated-wall cases for η greater than approximately $[f_{\eta\eta}(0)A]^{\frac{1}{2}}$. The results needed to find the principal boundary-layer properties appear in table 1 and figure 2.

In figures 2*a* and 2*b*; the variables $R(\infty)$ and $f_{\eta\eta}(0)$ are presented through use of normalized functions F_1 and F_2 where

$$F_1 \equiv \frac{R(\infty)-1}{\Lambda}\left\{\frac{8Pr[1+\log_{10}(1+\Lambda)]}{(Pr+3g_w)(Pr+g_w)}\right\}^{\frac{1}{2}}, \tag{4.1}$$

$$F_2 \equiv \frac{\{f_{\eta\eta}(0)[R(\infty)]^{\frac{1}{2}}-[f_{\eta\eta}(0)]_{\Lambda=0}\}[1+\log_{10}(1+\Lambda)]}{\Lambda(Pr+3g_w)/4}. \tag{4.2}$$

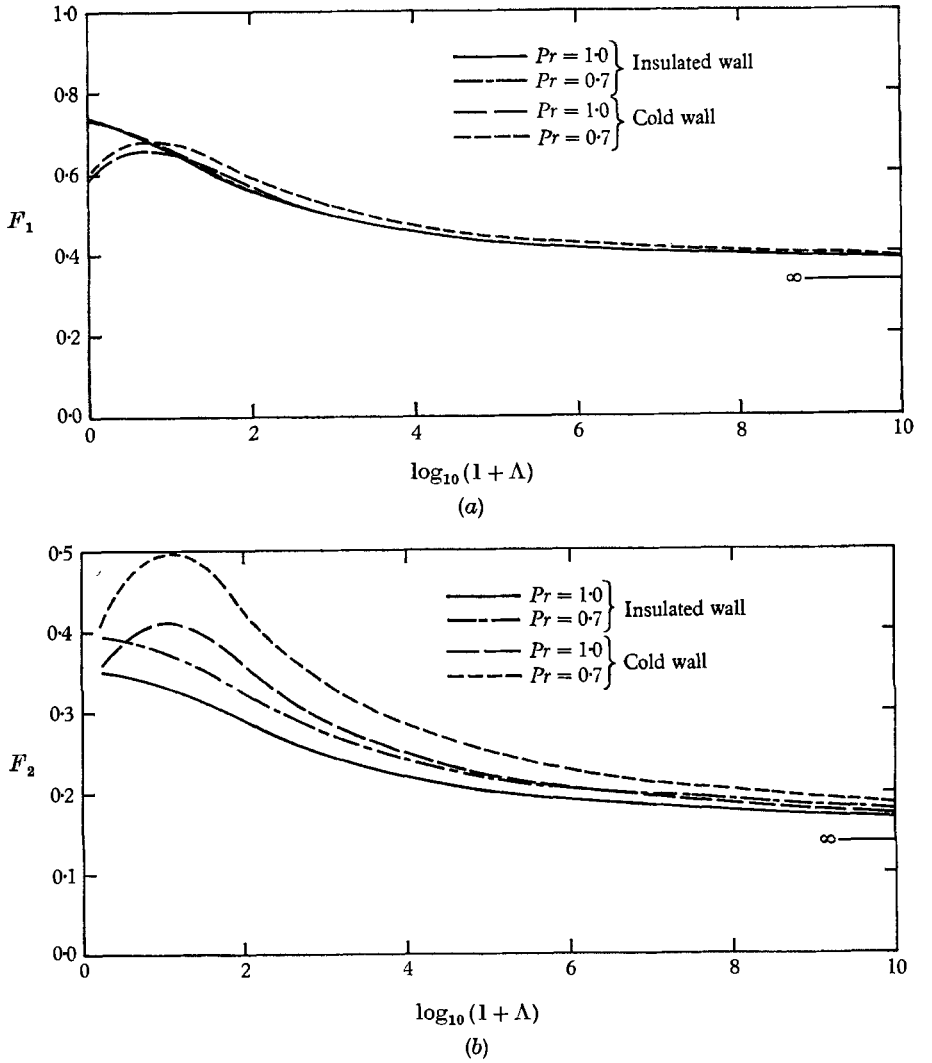

FIGURE 2. Self-similar hypersonic flow over slender axisymmetric body ($r_w \sim x^{\frac{3}{4}}$, $\omega = 1$, $\gamma = 7/5$). (*a*) Skin friction parameter, F_1 [equation (4.1)]. (*b*) Displacement thickness parameter, F_2 [equation (4.2)]. (*c*) Drag coefficient. (*d*) Velocity and stagnation enthalpy profiles near wall.

These functions were chosen so as to produce ordinates of order one for all degrees of interaction. The close grouping of curves in these figures means that principal flow properties can now be predicted with an interpolation error of less than 10 % given arbitrary Λ, Pr, and either g_w or $g_\eta(0)$. Figure 2*c* shows the very large

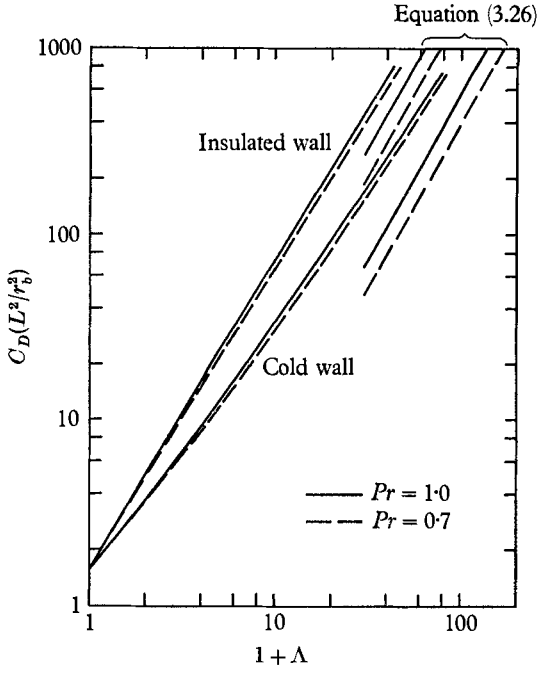

(*c*)

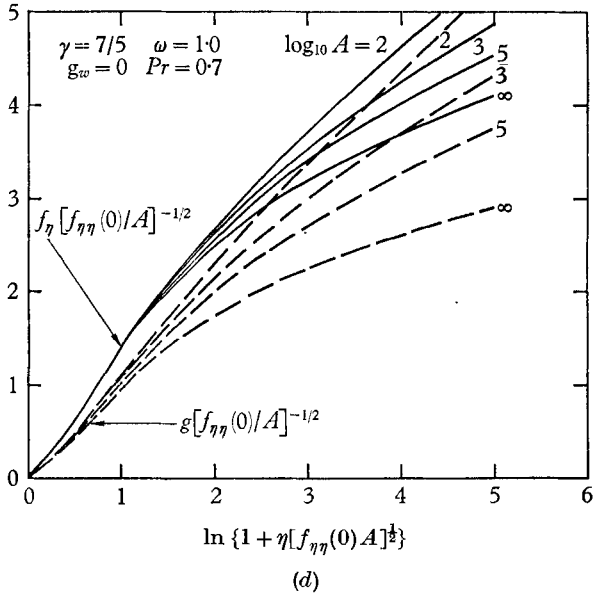

(*d*)

FIGURE 2. For legend see facing page.

increase in drag coefficient with Λ predicted by the present calculations and theory. Figure 2*d* exhibits cold-wall boundary-layer profiles near the wall for $Pr = 0{\cdot}7$, $\omega = 1$, $\gamma = \frac{7}{5}$, and $A \geqslant 100$. Similar curves for the case of an insulated wall depart from the strong-interaction profiles, (3.3) and (3.5), by less than 10 % for $A \geqslant 100$.

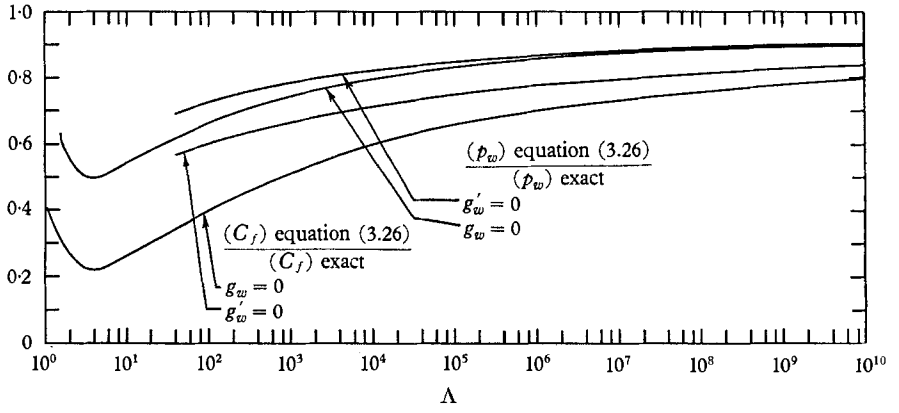

FIGURE 3. Ratio of asymptotic strong-interaction solution [equation (3.26)] to exact solution (table 1) for three-quarter power-law bodies ($Pr = 0{\cdot}7$, $\gamma = 1{\cdot}4$, $\omega = 1$).

In figure 3 is shown the ratio of pressure and skin friction coefficient from the strong-interaction theory, (3.26), to exact values (table 1) for three-quarter power-law bodies and $Pr = 0{\cdot}7$ ($\omega = 1$, $\gamma = \frac{7}{5}$). These errors are comparable with the theoretical error $\epsilon \sim (\log \Lambda)^{-\frac{1}{2}}$ for $\omega = 1$. Although the convergence of the theory as $\Lambda \to \infty$ is slow, the errors remain of order one for $\Lambda > 1$.

5. Discussion

The present axisymmetric strong-interaction theory represents an extension, to values of Pr and ω other than one, of Stewartson's (1964) theory for a model gas. Unlike Stewartson, the major boundary-layer properties have been obtained without recourse to numerical integrations. The outstanding feature of axisymmetric strong-interaction theory is its uniquely slow rate of convergence in the interaction parameter; namely, its error $\sim (\log \Lambda)^{-1/(\omega+1)}$. It has been seen in figure 3 that even for $A = 10^5 (\Lambda \sim 10^9)$ the error in the axisymmetric strong-interaction theory ranged up to 20 %. Appendix A shows that the theory has a domain of validity that is too restrictive for most practical applications. The theory does suggest ways of interpolating numerical data for interactions of only moderate strength (as in §4) and does provide starting values for numerical integrations of finite-interaction equations for sharp bodies. It also determines the reference temperature to improve solutions employing a linear-viscosity approximation.

For bodies which grow as x^n where $n < \frac{3}{4}$, Λ increases with x and strong interaction occurs downstream, if at all. If $n > \frac{3}{4}$, the interaction is strongest near the nose. For $n = \frac{3}{4}$, the interaction parameter Λ is independent of x.

Finally, some remarks concerning parameters and terminology are in order. It is important to distinguish three parameters when considering hypersonic viscous interaction on axisymmetric bodies. These are a shock strength parameter $(M_\infty dr_e/dx)^2$, a transverse curvature parameter δ/r_w and a 'pressure' interaction parameter $p_w/(p_w)_i$ where p_w is the local surface pressure and $(p_w)_i$ is the corresponding value for inviscid flow. The latter parameter defines the degree of viscous interaction. In the present study, it was assumed that the shock is always strong, $(M_\infty dr_e/dx)^2 \gg 1$. As a result, the single parameter Λ characterizes both the magnitude of the transverse curvature δ/r_w and the viscous interaction $p_w/(p_w)_i$. For more moderate shock strength, large values of δ/r_w need not imply a strong interaction (e.g. the flow far downstream of the nose of a cylindrical body). For two-dimensional flows, the transverse curvature parameter does not apply. In the special case of a flat plate, and only in this case, the shock strength and the degree of viscous interaction are both characterized by the familiar parameter $M_\infty^{2+\omega}(\nu_\infty/u_\infty x)^{\frac{1}{2}}$.

This work was supported by the United States Air Force under Contract no. F04695-67-C-0158. The authors gratefully acknowledge stimulating discussions and critical review by Professor H. K. Cheng of the University of Southern California. The numerical solutions were obtained by E. H. Fletcher, Aerospace Corporation.

Appendix A. Validity of strong interaction solution

This appendix translates the assumptions of strong interaction, continuum flow, no vorticity interaction, strong shock, and sharp nose into requirements on free-stream Mach number, Reynolds number, body slenderness, and nose thickness. The present theory is believed valid for arbitrary positive values of the parameters ω, Pr, $\gamma-1$ and g_w.

Rarefaction effects such as surface slip and temperature jump have been neglected. The local ratio $\mathscr{R}$ of mean free path to an appropriate characteristic thickness is taken as a measure of these effects. Although the mean free path reaches a maximum where the temperature peaks—viz. in the inner viscous layer at a velocity ratio $(Pr-g_w)/(2Pr)$, from (3.4) and (3.22a)—the ratio $\mathscr{R}$ may be greater at the wall than at the maximum temperature location (figure 1). At the wall, the characteristic thickness is taken to be the ratio of u_∞ to $(\partial u/\partial r)_w$, and it is easily shown that

$$\mathscr{R}_w \sim \frac{(\rho u)_\infty}{(\rho a)_w} C_f \sim \left[\frac{g_w \Lambda M_\infty^\omega Re_{x,\infty}^{-\frac{1}{2}}}{\log \Lambda}\right]^{\frac{1}{2}}, \tag{A 1}$$

where a is the speed of sound and $Re_{x,\infty} \equiv u_\infty x/\nu_\infty$. At the maximum temperature location, the characteristic thickness is the square root of the local ratio of h to d^2h/dr^2, which is of the same order as the local value of dr/df_η, found from (3.5). If $\mathscr{R}$ there is denoted as $\mathscr{R}_{MT}$,

$$\mathscr{R}_{MT} \sim [\Lambda^{1-(J_{MT}/J)} (\log \Lambda)^{-1} M_\infty^\omega Re_{x,\infty}^{-\frac{1}{2}}]^{\frac{1}{2}}, \tag{A 2}$$

where

$$J_{MT} \equiv \int_0^{(Pr-g_w)/(2Pr)} (g_w + Prt)^\omega (1-t)^\omega dt.$$

Comparison of (A 1) and (A 2) reveals that $\mathscr{R}_w > \mathscr{R}_{MT}$, that is, slip and temperature jump are the dominant rarefaction effect, whenever $g_w > \Lambda^{-J_{MT}/J}$.

Errors at the outer edge of the boundary layer can be grouped under the label of shock-wave heating and vorticity. At hypersonic speeds, the mass flux in the two viscous layers is very small, so that streamlines entering the boundary layer previously have crossed the shock wave far upstream near the leading edge, where the shock has relatively more slope and is highly curved. As a result, the effect of vorticity and the levels of entropy and M^{-2} (i.e. shock heating effects) at the outer edge of the convective layer may not be negligible. Lees (1956*b*) has shown for strong viscous interaction in plane flow that errors due to these effects are of order $(M_\infty^\omega Re_{x,\infty}^{-\frac{1}{2}})^k$, where, for $\omega = 1$, k is the proper fraction $1-2/(3\gamma)$. For axisymmetric strong interactions, the order of these effects is again a fractional power of $M_\infty^\omega Re_{x,\infty}^{-\frac{1}{2}}$, a power that depends on γ and ω.†

Whereas neglecting shock heating errors requires only that a power of $M_\infty^\omega Re_{x,\infty}^{-\frac{1}{2}}$ be small, neglecting either rarefaction errors (A 1) or (A 2) requires that $M_\infty^\omega Re_{x,\infty}^{-\frac{1}{2}}$ be exponentially small, since for the viscous interaction to be strong ($\epsilon \ll 1$), Λ must be exponentially large. It is this combined requirement of strong interaction and continuum flow that is hard to satisfy in practice, and hence upstream departures from the strong interaction theory are always dominated by rarefaction effects at or near the wall. For slender axisymmetric bodies the shock-heating error becomes as important as the rarefaction error when the viscous interaction is of *moderate* strength in the sense $\log \Lambda = O(1)$, in which case the shock-wave shape and the exponent k depend on body shape as well as on γ and ω.

Three other parameters must also be exponentially small in ϵ. These are r_w^2/x^2, M_∞^{-2} and d/x, where d is a nose-thickness dimension. r_w^2/x^2 is just the ratio of $M_\infty^\omega Re_{x,\infty}^{-\frac{1}{2}}$, which must be exponentially small, and Λ, which must be exponentially large. The requirement on M_∞^{-2} is obtained by observing that the product of M_∞^2 and $M_\infty^\omega Re_{x,\infty}^{-\frac{1}{2}}$ is the shock strength parameter, which must be large. Finally, the nose drag is negligible compared with the viscous drag only if d/x is much less than the exponentially small product $M_\infty^\omega (Re_{x,\infty} \log \Lambda)^{-\frac{1}{2}}$.

Despite these constraints on the present theory, it can be used to identify trends with Pr, g_w, γ and ω, to provide starting values near the nose for continuum-flow models where $n(0) > \frac{3}{4}$, and to establish the linear-viscosity approximation (3.32).

REFERENCES

Bush, W. B. 1966 *J. Fluid Mech.* **25**, 51.

Cheng, H. K., Hall, J. G., Golian, T. C. & Hertzberg, A. 1961 *J. Aerospace Sci.* **28**, 353.

Chernyi, G. G. 1961 *Introduction to Hypersonic Flow* (trans. and ed. R. F. Probstein). New York: Academic Press.

Glauert, M. B. & Lighthill, M. J. 1950 *Proc. Roy. Soc.* A **230**, 188.

Hayes, W. D. & Probstein, R. F. 1966 *Hypersonic Flow Theory*, 2nd ed., vol I. New York: Academic Press.

Lees, L. 1956*a* *Jet Propulsion*, **26**, 259, 274.

† R. S. Lee, private communication.

LEES, L. 1956*b* *J. Aero. Sci.* **23**, 594, 612.

MOORE, F. K. 1952 *Nat. Adv. Comm. Aero. Tech. Note, NACA TN* 2722.

SOLOMON, J. M. 1967 U.S. Naval Ordinance Laboratory, White Oak, Md., NOLTR 66-225.

STEWARTSON, K. 1955 *Quart. Appl. Math.* **13**, 113.

STEWARTSON, K. 1964 *Phys. Fluids*, **7**, 667; **7**, 2025.

YASUHARA, M. 1956 *J. Phys. Soc. Japan*, **11**, 878.

YASUHARA, M. 1962 *J. Aerospace Sci.* **29**, 667, 688.